University of Huddersfield Repository

Khwandah, Sinan, Cosmas, John, Glover, Ian, Lazaridis, Pavlos, Prasad, Neeli and Zaharis, Zaharias D.

Direct and External Intensity Modulation in OFDM RoF Links

Original Citation

This version is available at http://eprints.hud.ac.uk/id/eprint/25564/

http://eprints.hud.ac.uk/

Direct and External Intensity Modulation in OFDM RoF Links

Sinan A. Khwandah
John P. Cosmas
Ian A. Glover
Pavlos I. Lazaridis
Neeli R. Prasad
Zaharias D. Zaharis
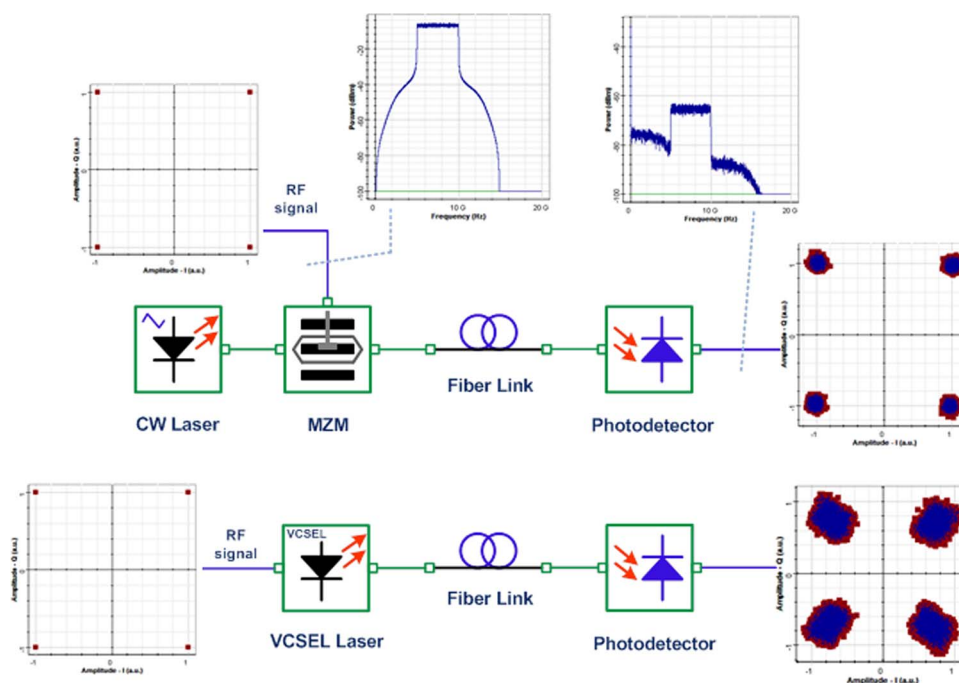
Direct and External Intensity Modulation in OFDM RoF Links

Sinan A. Khwandah,[1] **John P. Cosmas,**[1] **Ian A. Glover,**[2] **Pavlos I. Lazaridis,**[2] **Neeli R. Prasad,**[3] **and Zaharias D. Zaharis**[4]

[1]Department of Electronic and Computer Engineering, College of Engineering, Design and Physical Sciences, Brunel University London, Uxbridge UB8 3PH, U.K.
[2]Department of Engineering and Technology, University of Huddersfield, Huddersfield HD1 3DH, U.K.
[3]Center for TeleInFrastructure (CTIF) Aalborg University, 9220 Aalborg East, Denmark
[4]Department of Electrical and Computer Engineering, Aristotle University of Thessaloniki, 54124 Thessaloniki, Greece

Abstract: Radio-over-fiber (RoF) systems comprise light modulation and transmission of millimeter-wave signals over fiber links. The aim of this study is to investigate the performance of external and direct intensity modulation in RoF links and to analyze the drawbacks induced by different components of the optical system. In external modulation, the Mach–Zehnder modulator (MZM) is used, whereas the vertical-cavity surface-emitting laser (VCSEL) is utilized in direct modulation. Both modulation schemes are tested for a vector modulation format, i.e., the quadrature amplitude modulation (QAM), where an orthogonal frequency-division multiplexing (OFDM) scheme is used to generate signal subcarriers. The simulations are carried out with the same values of common global parameters for both schemes of intensity modulation. Although VCSEL is a promising device for future RoF systems, the external modulation shows a more robust performance compared with that of VCSEL when implemented with the OFDM modulation technique.

Index Terms: Radio-over-fiber (RoF), vertical-cavity surface-emitting laser (VCSEL), Mach–Zehnder modulator (MZM), external intensity modulation, direct intensity modulation, optical orthogonal frequency-division multiplexing (OFDM).

1. Introduction

There has been a remarkable growth in the deployment of analog optical links due to their capabilities and advantages for a wide range of applications such as antenna remoting, radio over fiber (RoF), and optical signal processing [1]. Networks can use light to transmit data, instead of electronic transmission through cables, so that today, optical technology contributes to all communication networks and has real applications. The new wavelength division multiplexing (WDM) technology enables large capacities of tens of terabits per second (Tbps) using a single fiber line [2]. This has made optical networks more flexible and able to meet high data rate demands for broadband services, which require more spectral bandwidth and higher frequencies, in the range of Gigabits per second (Gbps).

Recent research has focused on enhancing the performance of opto-electric links, and on finding a solution to overcome existing limitations and impairments, which occur throughout the link and degrade the performance of the main processes. These limitations include the adverse
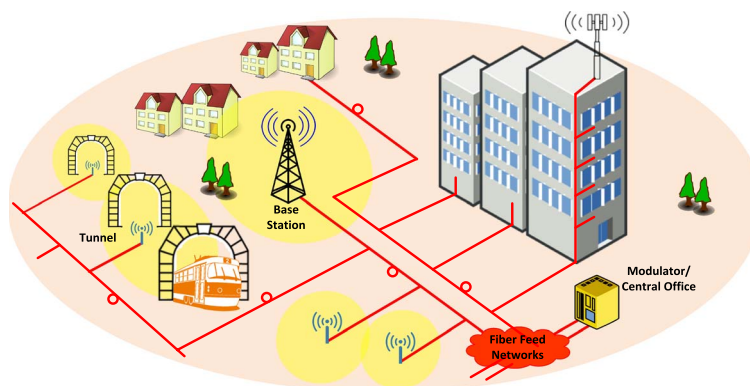
Fig. 1. Millimeter-wave fiber-wireless network.

effects of electronic-optical conversion at the transmitter, and optical-electronic conversion at the receiver, in addition to the effects of the optical fiber on the transmitted light wave such as chromatic dispersion and non-linearity.

1.1. Optical-Wireless Integration

Optical intensity modulation is a type of modulation where the optical power of a light source is modulated according to a modulating signal (RF signal) in order to allow electrical signals to be transmitted over an optical carrier. Before RoF systems were introduced, the processing of signals took place in the base station and the signals were distributed directly to the connected antennas. The generic architecture of a millimeter-wave (mm-wave) fiber-wireless architecture is shown in Fig. 1, where the radio frequency signals are distributed from the Central Office or Headend to remote antenna units. This offers more flexibility and simplicity at the base station side since all the overheads of processing, modulation and maintenance are moved to a central location and then the optical signals are distributed through low-loss optical fibers [3]. At the antenna side, there are only opto-electronic converters and amplifiers.

When radio signals are transmitted in free space, they undergo attenuation due to reflection and absorption by the atmosphere, and these losses and effects increase more when the frequency is higher. Also, transmission of mm-waves through traditional transmission lines is not practical as it requires down-conversion of high frequencies to intermediate frequencies or basebands, and then up-conversion after transmission.

New technologies such as WDM, Dense WDM and optical time-division multiplexing (OTDM) are expected to provide larger bandwidth using optical fibers. This large optical bandwidth allows us to develop novel signal processing in the optical domain (which is simply not possible in the electrical domain), such as optical amplifying and filtering, with simpler and cheaper optical components which are protected against interference from electromagnetic fields [4]. The electrical signal is converted to an optical one, processed optically, and then converted back to an electrical signal.

Optical wavelengths which correspond to the lowest attenuation are 850 nm, 1310 nm, and 1550 nm. Traditional optical fibers are capable of supporting a large theoretical bandwidth of 50 THz by combining the transmitting windows of 1310 nm, and 1550 nm together [5]. The preferred optical wavelength is around 1550 nm ($\sim$193.1 THz) because this corresponds to the lowest power attenuation figure of the three wavelengths when light propagates throughout the fiber link. Further improvements to loss reduction are still being achieved, although this has been proved to be difficult with fiber fabrication techniques [6], [7].

1.2. The Optical Challenges

The millimeter-wave spectrum (30–300 GHz or 10-1 mm-wavelength) is classified as extremely high frequency (EHF) [8]. The spectrum of the optical signal is wider than that of the RF

signal, due to the modulation process which produces harmonics on both sides of the optical carrier. The mm-wave, which is optically modulated, undergoes different impairments while propagating within an optical link; due to the non-linearity of the electrical-optical modulator, the efficiency of the modulating process results in weak optical signals converted from mm-wave wireless signals.

The properties of the dispersive material affect the waves of different frequencies and make them travel with different speeds. This has been known as chromatic dispersion (CD) in the fiber link and causes distortions in the signals over long distances where different components of the signal have different arrival time delays and different amplitude attenuations [9].

In order to improve the performance of the link, the optical impairment and several challenging issues such as noise and distortion must be considered carefully. Noise causes fluctuations in the optical power produced by the laser diode. The noise produced at the input reaches the receiver either amplified or degraded. Any Ohmic impedance (at the modulator, laser diode, or photo-detector side) generates thermal noise. If the link has no gain, the thermal noise at the photo-detector dominates.

Distortion exists in the link only when the signal is present, while noise exists with or without the signal. The main cause of distortion is the non-linearity and it is accompanied by the generation of new frequencies at the output. Non-linearity causes a pure sinusoid wave (*f-frequency*) with infinite harmonics to appear, starting from the DC component (*0-frequency*), Fundamental (*f*), Second-order ($f_1 \pm f_2$), Third-order ($2f_1 \pm f_2, 2f_2 \pm f_1$), and so on [10].

The losses in fiber link increase slowly compared to a dramatic increase in a coaxial cable. However, there are RF-optical conversion impairments in the modulation and photo-detection processes. Therefore, in RoF systems, issues such as light modulation, coupling light into fibers and photo-detection processes have the largest impact on the system's performance. However, there are many limiting factors such as chirping, which is a type of unwanted modulation which happens to the optical power and is associated with the main modulation process; also, it causes an increase in the dispersion effects of optical fiber and intersymbol interference (ISI) when the signal is transmitted through long optical fiber [11].

2. Optical OFDM Analysis

OFDM modulation has been adapted into a wide range of applications in wireless systems due to its high spectral efficiency and its advantages in the RF domain. Recently, optical OFDM has attracted much attention as a promising technology for future optical communications. Therefore, optical technology aims to benefit from OFDM's advantages [12].

The time-domain electrical waveform for one OFDM symbol, which consists of N_{sc} subcarriers, is represented by $S(t)$

$$S(t) \sum_{k=0}^{N_{SC}-1} C_k e^{j2\pi f_k t} \tag{1}$$

where C_k is the OFDM information symbol for the kth subcarrier, and f_k is the frequency of the subcarrier. The optical OFDM signal is described by

$$S_0(t) = e^{j2\pi f_o t} + \alpha e^{j2\pi(f_0+\Delta f)t} \sum_{k=0}^{N_{SC}-1} C_k e^{j2\pi f_k t} \tag{2}$$

where f_o is the frequency of the optical carrier, and α is a scaling coefficient which describes the OFDM signal strength with reference to the main carrier [13]. Δf is the guard band between the optical carrier and the OFDM band. The guard band is required because the electrical field of the optical signal is usually not a linear replica of the baseband signal, and it is therefore protected from interference caused by second-order products as shown below [14].

The effect of chromatic dispersion during transmission over fiber is represented by a phase delay $\phi(t)$ in the received signal which is the continuous-time filtered optical OFDM symbol,
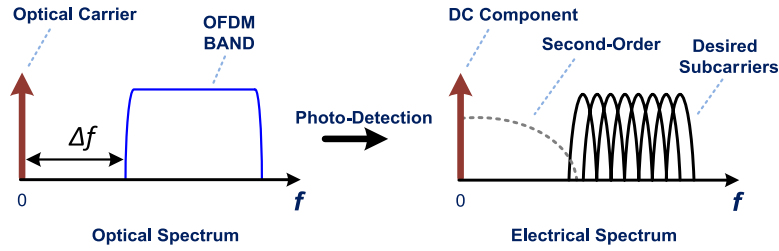
Fig. 2. Received OFDM spectrum.

including both the optical carrier and data subcarriers. Also, in addition to chromatic dispersion, the amplified spontaneous emission (ASE) noise is added to the signal after it passes through the optical amplifier. The ASE noise is due to photons spontaneously emitted by active ions and contributes significantly to the total noise of the amplified signal [15].

For simplicity, the transfer functions from the transmitter to receiver are not shown in the following equation of the optical signal $R(t)$ arriving at the photo-detector:

$$R(t) = e^{j(2\pi f_o t + \phi(t))} + \alpha e^{j(2\pi (f_0 + \Delta f)t + \phi(t))} \sum_{k=0}^{N_{SC}-1} C_k \, e^{j2\pi f_k t} + n_{ASE}(t) \tag{3}$$

$$R(t) = R_S(t) + R_N(t). \tag{4}$$

The first two terms in (3) represent the received signal $R_s(t)$ corrupted by the additive noise $R_N(t)$ which is the ASE noise due to the optical amplification. The photo-detector is modeled as an ideal square law device; the produced photocurrent is proportional to $|R(t)|^2$. Therefore when the photodetector responds to the square of the optical field this gives the useful part $|R_s(t)|^2$ and the noise products

$$|R(t)|^2 = |R_S(t) + R_N(t)|^2 = |R_S(t)|^2 + 2R_S(t).R_N(t) + |R_N(t)|^2 \tag{5}$$

$$|R_S(t)|^2 = R_S(t).R_S^*(t) \tag{6}$$

$$|R(t)|^2 = 1 + 2\alpha \, \mathrm{Re}\left\{ e^{j2\pi \Delta f t} \sum_{k=1}^{N_{SC}-1} C_k \, e^{j2\pi f_k t} \right\} + \alpha^2 \sum_{k_1=0}^{N_{SC}-1} \sum_{k_2=0}^{N_{SC}-1} C_{k_1} C_{k_2}^* e^{j2\pi (f_{k_1} - f_{k_2})t}$$
$$+ n_{SABN}(t) + n_{AABN}(t) + n_{CABN}(t) \tag{7}$$

where in (7), $*$ is the complex conjugate, and the term 1 represents the DC component which can be removed by filtering. The second term is the fundamental (f_k) and represents the desired OFDM subcarriers. The third term represents the second-order product $(f_{k_1} - f_{k_2})$ which is unwanted distortion and appears near the DC component; its amplitudes decrease with frequency. The second-order product causes interference when it overlaps with the detected desired OFDM band. Fig. 2 shows that the guard band protects the data subcarriers so that the desired subcarriers can be obtained without being interfered with by the second-order components.

The noise products—known as the electrical beat noises—are: the signal-ASE beat noise $n_{SABN}(t)$ between the signal and the ASE frequency components (product of the term $2R_s(t)R_n(t)$), and the ASE-ASE beat noise $n_{AABN}(t)$ between each frequency component of the ASE with itself (product of $|R_n(t)|^2$). There is also the carrier-ASE beat noise $n_{CABN}(t)$. These electrical beat noises have been studied in [16].

In order to reduce the out-of-band ASE noise, an optical filter is used after the optical amplifier. The optical filter shapes the power spectral density (PSD) of the ASE noise so that it can be treated before beating at the photo-diode.
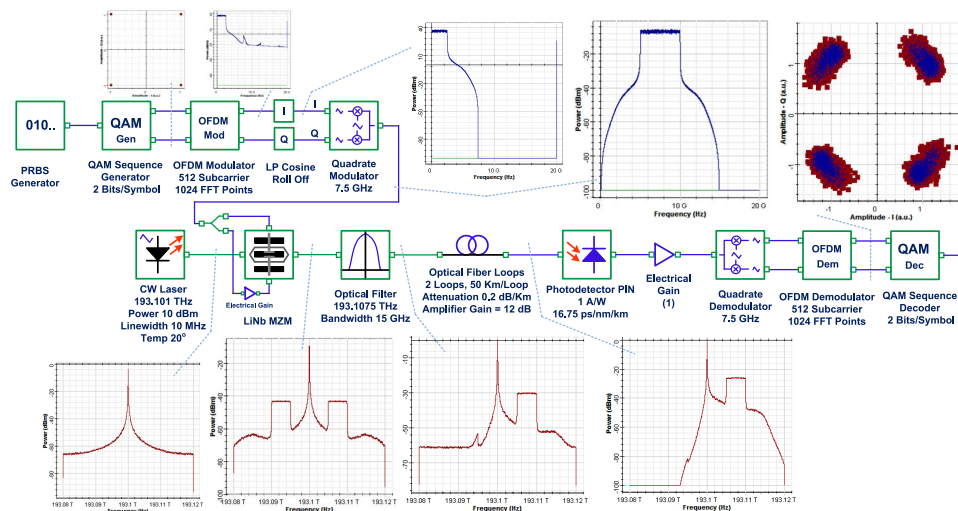
Fig. 3. External modulation of 4-QAM OFDM.

3. Simulations Setup and Results

The Optisystem software is used here to simulate the optical communication experiments. The system performance is presented through visualizing tools, such as optical spectrum analyzer, RF spectrum analyzer, and constellation visualizer, which are used to display the spectrum at the output of the circuit components. Fig. 3 shows a 4-QAM OFDM external modulation circuit as well as the modulated and the recovered signals. In QAM-OFDM, the random bit sequence is fed into the M-QAM generator to produce M-Array sequences, with I and Q outputs. Next, I and Q outputs are fed into an OFDM modulator to transmit the QAM symbols over parallel overlapped orthogonal subcarriers. Then a quadrature modulator is used to modulate its I and Q electrical inputs by RF carriers of 7.5 GHz.

The result of the intensity modulation is an optical carrier with a double-sideband (ODSB). The optical spectrum at the output of the Mach–Zehnder Modulator (MZM) is symmetric and centered around 193.1 THz. The optical spectrum is spread over a wide range of frequencies which affects the quality of the signal when it is transmitted over the optical fiber link. The two sidebands produce two beats at the receiver and these two beats combine to form the RF signal. However, when the ODSB signal propagates through the optical fiber, chromatic dispersion causes a relative phase difference between the sidebands and the optical carrier. At the photodetector, the square-law process gives two components which are shifted in phase with respect to the carrier and this causes degradation in the output RF power. The effects of chromatic dispersion can be reduced by eliminating one of the sidebands of the DSB optical spectrum. An optical filter is used to suppress one of the sidebands in order to reduce the effects of chromatic dispersion. During the transmission within the optical fiber loops, the single sideband—with carrier—signal is amplified and filtered several times and is then delivered to the photodetector at the end of the transmission.

At the receiver, the opposite logic is used to demodulate and recover the signal. The quadrate demodulator duplicates the electrical input signal, multiplies it by sine and cosine carriers and then applies a low pass filtering process. The OFDM demodulator removes the guard periods then applies the FFT process for each OFDM symbol and regenerates the transmitted spectrum. The QAM decoder decodes the two M-Array inputs into one binary output.

Both the complexity and high cost of the external modulation make it necessary to find new schemes, which offer simplicity and low cost. The laser diode is easy to test, is small, requires less power to operate, and is cheap to manufacture. The direct modulation is actually a simple scheme and the VCSEL emits a narrow and directional beam compared to other directly
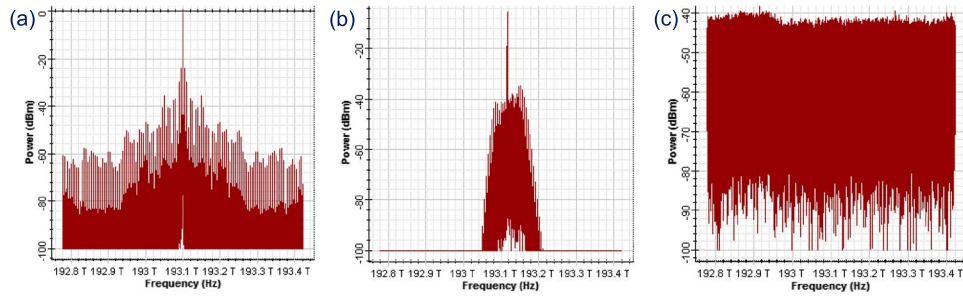
Fig. 4. Spectrum of (a) directly modulated laser, (b) VCSEL, and (c) saturated VCSEL.
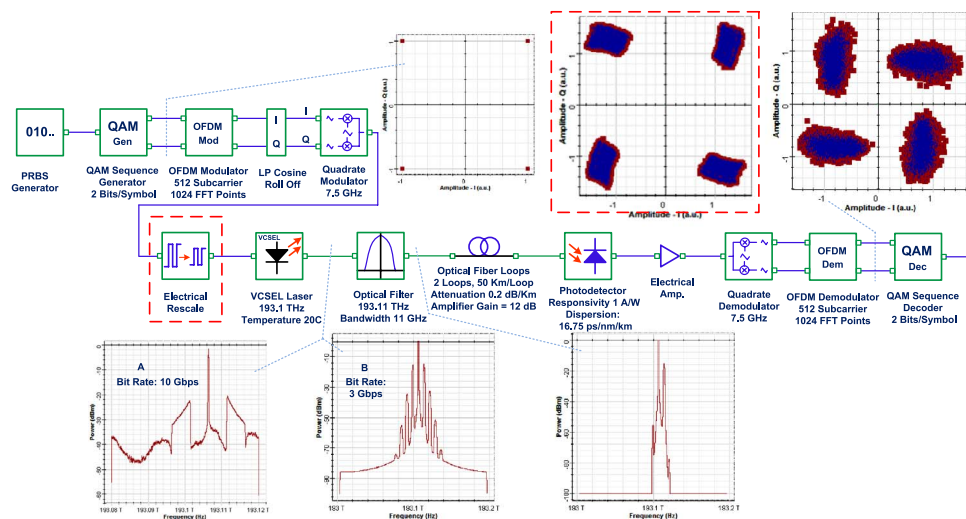

Fig. 5. Direct modulation of 4-QAM OFDM.

modulated laser diodes (that have wide and isotropic emission) (see Fig. 4). The narrow beam is suitable, more efficient and easier for fiber coupling with less power loss. Moreover, a narrow beam is less affected by fiber impairments than a wider one and requires less filtering. Therefore, the VCSEL is used for direct modulation, as shown in Fig. 5, while the global parameters are the same as in the external modulation setup.

Fig. 5 shows the direct modulation scheme, where the RF signal is applied directly to the VCSEL to modulate its optical density, and the parameters of the optical filter following the VCSEL are changed in order to implement a pass band compatible with the optical carrier and the upper side band.

The optical spectrum of the VCSEL is not completely symmetric (see Fig. 5), while the optical spectrum produced by the MZM in an external modulation scheme is perfectly symmetric (see Fig. 3). The optical carrier is centered around 193.106 THz, while on the other hand, the optical carrier in the spectrum of the MZM is centered on 193.1 THz, with upper and lower sidebands located at 193.1075 and 193.0925 THz, respectively.

One important issue is the bit rate at the input of the VCSEL. Due to the bandwidth limitation of the employed VCSEL, the bit rate is reduced to 3 Gbps. It is necessary to reduce the bit rate because VCSEL is a diode and is therefore affected by the carrier recovery time like every semiconductor. The carrier recovery time is an important factor to be considered when using semiconductor materials with high data rates; when the data rate increases, the input signal frequency increases too. As a result, the capacitor effect becomes dominant and impacts negatively both the bandwidth of the laser diode and the recovery time of the carriers, degrading in
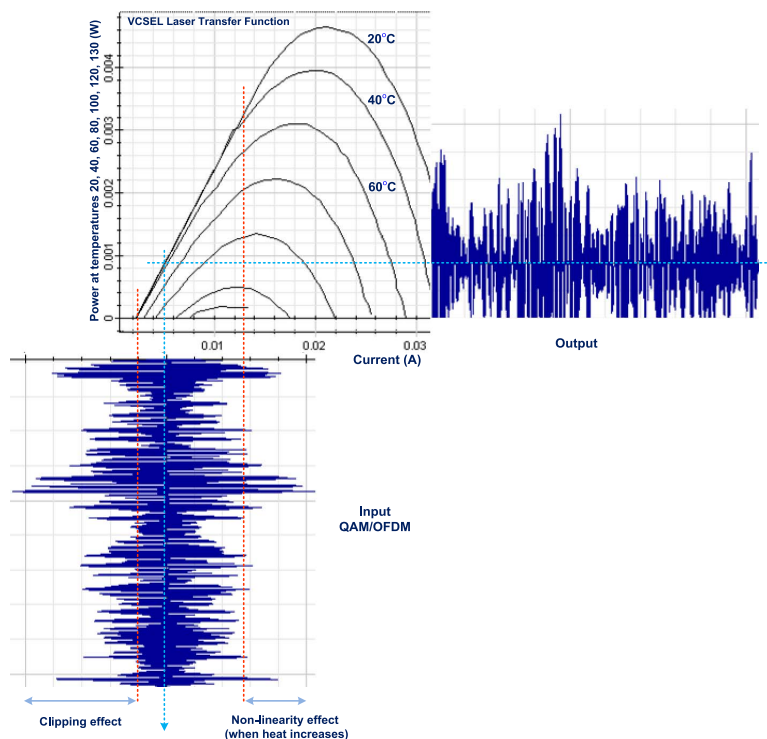
Fig. 6. Clipping and non-linearity effects in direct modulation scheme.

this way the performance of the laser diode. The progress of VCSEL products must keep track with the networks' ever growing bit rates, and recently, certain types of VCSELs have been man-ufactured to operate at high bit rates of up to tens of Gbps, as well as at high temperatures [17].

If we examine the new spectrum at the output of the VCSEL (see Fig. 5 spectrum case B), we find that, firstly, the spectrum symmetry is improved but not centered at 193.1 THz and, sec-ondly, it contains adjacent harmonics. The correct source power before the VCSEL is important, since a high-power input signal causes VCSEL saturation [see Fig. 4(c)]. Also, by keeping the source power at low levels, we may reduce the power of the harmonics at the VCSEL output to a certain level, which helps to alleviate their effects and also to determine the filter's parameters. Adjacent harmonics make it difficult to set the frequency and the bandwidth of the filter in a way that maintains the carrier and suppresses only one of the sidebands. By the end, there will be residual harmonics which will be transferred over the fiber. However, the power difference be-tween the residual harmonics and the remaining sideband will be more than 30 dB; therefore, the effects and the potential for errors are tolerable. At the output, the level of signal distortion and the level of noise are high; this is due to the previously-described process.

Another issue considered here, that concerns the use of OFDM with the direct modulation scheme, is the high values of the peak-to-average power ratio (PAPR) of the OFDM signal. This is considered to be a main drawback of the use of OFDM in digital communication, since it causes distortions at the transmitter side. When OFDM is applied in RF systems, the semicon-ductor devices saturate due to high PAPR values. This is also a challenge in optical systems due to the non-linearity of amplifiers, laser diodes, and optical fibers. The high PAPR values in OFDM signals are related to the use of a large number of subcarriers. In some cases, the peak value, which depends on the number of subcarriers, is greater than 20 times the average value. Fig. 6 shows the LI curve of a VCSEL for different temperature values [18] while the VCSEL is biased at 5 mA. In order to avoid non-linearity in the gain and saturation at 20 °C, the bias cur-rent should not exceed 5mA. However, the temperature is more likely to become greater than 20 °C due to self-heating of the device, which again results in a non-linear response. When the
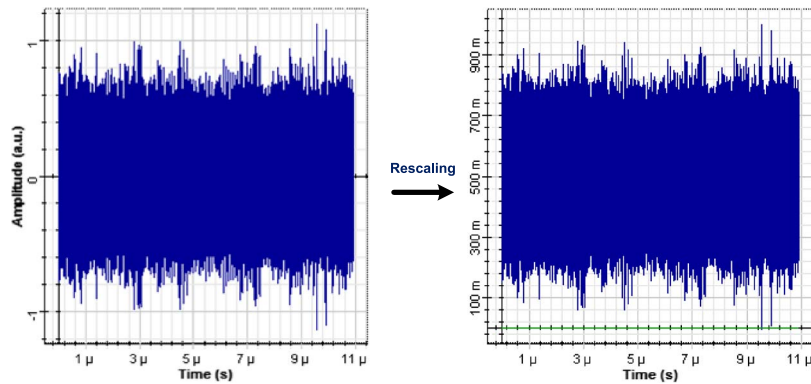
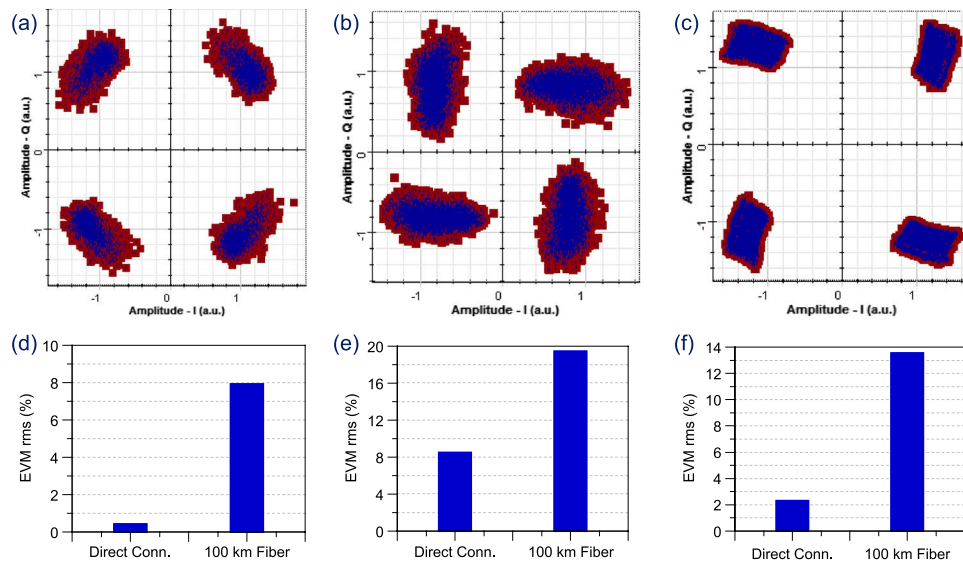Fig. 7. Electrical rescaling of the QAM/OFDM signal.

Fig. 8. (a) External modulation. (b) Direct modulation. (c) Direct modulation after OFDM rescaling. (d) EVM of external modulation. (e) EVM of direct modulation. (f) EVM of direct modulation after OFDM rescaling.

OFDM signal is applied to the VCSEL, the signal undergoes clipping and non-linearity effects. The most damaging of these effects is clipping (see Fig. 6).

One simple method to reduce high PAPR values of OFDM signals is to electrically rescale the signal and shift it in order to get it positioned in the linear range of the curve of the VCSEL (see Fig. 7). Rescaling of the OFDM signal comprises the reduction of the signal total power and then an increase in the average power by adding a DC bias. The DC bias shifts the signal closer to the linear range. Fig. 8 (cases a, b and c) shows a comparison between the external and the direct modulation of the 4-QAM (QPSK) OFDM while the simulation is carried out over a 100 km fiber link, and in order to quantify the performance of the two modulation techniques, the error vector magnitude (EVM) is evaluated to give an indication of the signal distortion. The comparison is presented also for a direct connection, where the optical modulator and the photodetector are directly connected to show the effects of modulator imperfections. In the external modulation, the constellation diagram shows that the received symbols are better positioned than in the direct modulation, and this is quantified by the EVM results.

Table 1 shows that the direct connection at the output of the transmitter gives an EVM of 0.4% which is almost perfect (an ideal modulator would have 0%), and this value increases to 7.9%

TABLE 1

EVM (rms) of the simulated scenarios

Modulation	EVM – direct connection	EVM – after 100 Km Fiber
External (Mach-Zehnder)	0.4%	7.9%
Direct (VCSEL)	8.5%	19.4%
Direct (VCSEL) after rescaling	2.3%	13.5%

over a 100 km fiber link because of the fiber dispersion characteristics. Due to its non-linearity, the VCSEL has a higher EVM value, even in the direct connection case and this value increases from 8.5% to 19.4% after propagation over the 100 km fiber link. When signal rescaling is performed in order to position the signal variation in the linear range of the VCSEL, a lower EVM value is achieved either in the direct connection case (the value decreases from 8.5% to 2.3%) or in the 100 km fiber link case (the value decreases from 19.4% to 13.5%). Although there is an improvement in the EVM values when OFDM signal rescaling is applied, the signal appears to start wrapping, and this is due to the rollover of the VCSEL curve. This indicates that the applied signal is still out of the linear range the VCSEL. Thus, adding a DC bias may help when the number of OFDM signal subcarriers is small, but, when the number of subcarriers is high, the PAPR will become very high, and thus, shifting will not be efficient enough.

Another proposed method to reduce the PAPR is to clip the signal before it is applied to the VCSEL. Clipping removes the high-power peaks of the signal, without changing its phase. This is done by multiplying the signal by a predetermined threshold. However, this causes clipping loss and leads to out-of-band spectral regrowth and additional in-band distortion. Therefore, BER may increase and filtering is needed. Clipping in the time domain has been proposed in several approaches such as in [19], where asymmetrically clipped optical OFDM with recoverable upper-clipping procedure is applied.

On the other hand, instead of applying time-domain clipping and filtering between the inverse fast Fourier transform (IFFT) stage and Cyclic-Prefix stage in the OFDM generator, clipping is proposed in the time domain while filtering is applied in the frequency domain to minimize the performance degradation due to clipping. This is the procedure followed in [20], where each OFDM symbol is modified by applying the clipping window on the time-domain symbols after the IFFT operation and then by applying FFT followed by filtering of the symbols in the frequency domain to get the OFDM symbol PAPR below a specified value. In this way, less distortion and lower out-of-band radiation are produced.

As mentioned previously, the exact bias of the VCSEL is very important and the bias current shifting is not a straightforward process since shifting towards the threshold current level causes clipping to appear and thus results in EVM increase (as shown in Fig. 6), while shifting towards a higher bias current also increases the EVM of signals with high PARP values due to entering into the non-linear range. VCSEL biasing in the linear range of the LI curve is studied in [21], where the optimum values of the bias current are investigated. The idea is based on finding a minimum EVM value which is a trade-off between minimum clipping effects and the desired modulation values. However, the thermal effect is a limiting factor that should be also considered when searching the optimum bias current, as self-heating of the device minimizes the linear range of the VCSEL and thus clipping and non-linearity effects are inevitable.

4. Conclusion

The direct and external intensity modulations in OFDM RoF systems have been presented and compared. The external modulation method exhibits better performance and produces a stable and symmetric spectrum. The error vector magnitude (EVM) values of the direct and external modulations have been obtained and compared. These values show that a much better modulation performance is produced by the external Mach–Zehnder modulator, while direct VCSEL laser diode modulation increases the EVM by 8% compared to the external modulator in the

direct connection case. Moreover, the EVM value further increases after propagation through a 100 km fiber link, which corresponds to a larger signal distortion of the signal constellation. Again, the results are much better for the more expensive external modulator. The high power of the signal degrades the performance of a VCSEL, which is better suited to lower amplitude modulation. Furthermore, it is shown that high data rates have an adverse impact on the VCSEL performance and on its optical spectrum symmetry. Techniques that can significantly lower VCSEL signal distortion such as rescaling have been discussed.

There are still several remaining issues that need to be resolved, in order to make the direct laser modulation as robust as the external modulation. Such an issue is the performance degradation of the direct modulation circuit due to high PAPR values of the OFDM signal and the non-linearity of the VCSEL.

References

[1] J. D. McKinney and K. J. Williams, "Sampled analog optical links," *IEEE Trans. Microw. Theory Techn.*, vol. 57, no. 8, pp. 2093–2099, Aug. 2009.

[2] R. C. Alferness, "The evolution of configurable wavelength multiplexed optical networks—A historical perspective," *Proc. IEEE*, vol. 100, no. 5, pp. 1023–1034, May 2012.

[3] C. Lim *et al.,* "Fiber-wireless networks and subsystem technologies," *J. Lightw. Technol.*, vol. 28, no. 4, pp. 390–405, Feb. 2010.

[4] A. E. Willner, S. Khaleghi, M. R. Chitgarha, and O. F. Yilmaz, "All-optical signal processing," *J. Lightw. Technol.*, vol. 32, no. 4, pp. 660–680, Feb. 2014.

[5] B. Mukherjee, "Enabling technologies: Building blocks," in *Optical WDM Networks,* Springer USA, 2006, pp. 43–44.

[6] J. P. R. Lacey, G. J. Pendock, and R. S. Tucker, "All-optical 1300-nm to 1550-nm wavelength conversion using cross-phase modulation in a semiconductor optical amplifier," *IEEE Photon. Technol. Lett.*, vol. 8, no. 7, pp. 885–887, Jul. 2002.

[7] Y. Wang *et al.,* "Hollow-core photonic crystal fibre for high power laser beam delivery," *High Power Laser Sci. Eng.*, vol. 1, no. 1, pp. 17–28, 2013.

[8] B. A. Khawaja and M. J. Cryan, "Characterization of multimode fibers for use in millimeter wave radio-over-fiber systems," *Microw. Opt. Technol. Lett.*, vol. 50, no. 8, pp. 2005–2007, Aug. 2008.

[9] R. B. Chaudhuri and A. Das Barman, "Mitigation of chromatic dispersion electronically in a coherent optical communication system," in *Proc. ICMAP*, 2013, pp. 1–5.

[10] C. H. Cox, *Analog Optical Links: Theory and Practice.* Cambridge, U.K.: Cambridge Univ. Press, 2006.

[11] *RP Photonics Encyclopedia/Chirp*, Dec. 2010. [Online]. Available: http://www.rp-photonics.com/chirp.html?s=ak

[12] J. Armstrong, "OFDM for optical communications," *J. Lightw. Technol.*, vol. 27, no. 3, pp. 189–204, Feb. 2009.

[13] S. A. Nezamalhosseini *et al.,* "Theoretical and experimental investigation of direct detection optical OFDM transmission using beat interference cancellation receiver," *Opt. Exp.*, vol. 21, no. 13, pp. 15 237–15 246, Jul. 2013.

[14] Q. Yang, A. Al Amin, and W. Shieh, "Optical OFDM basics," in *Proc. Impact Nonlinearities Fiber Opt. Commun. Anonymous Springer*, 2011, pp. 43–85.

[15] J. P. Dakin and R. G. Brown, *Handbook of Optoelectronics (Two-Volume Set).* Boca Raton, FL, USA: CRC, 2006.

[16] W.-R. Peng, K.-M. Feng, A. E. Willner, and S. Chi, "Estimation of the bit error rate for direct-detected OFDM signals with optically preamplified receivers," *J. Lightw. Technol.*, vol. 27, no. 10, pp. 1340–1346, May 2009.

[17] Vertically Integrated Systems, "Fiber optics components," VI Systems GmbH, Berlin, Germany, Tech. Rep. 140432-02, 2014.

[18] Optisystem Tutorials, "VCSEL laser measured LI curve iteration," Optiwave, Ottawa, ON, Canada, 2012.

[19] W. Xu, M. Wu, H. Zhang, X. You, and C. Zhao, "ACO-OFDM-specified recoverable upper clipping with efficient detection for optical wireless communications," *IEEE Photon. J.*, vol. 6, no. 5, pp. 1–17, Oct. 2014.

[20] Y. Wang and Z. Luo, "Optimized iterative clipping and filtering for PAPR reduction of OFDM signals," *IEEE Trans. Commun.*, vol. 59, no. 1, pp. 33–37, Jan. 2011.

[21] A. Schimpf, D. Bucci, and B. Cabon, "Optimum biasing of VCSEL diodes for all-optical up-conversion of OFDM signals," *J. Lightw. Technol.*, vol. 27, no. 16, pp. 3484–3489, Aug. 15, 2009.